

Federated Offline Reinforcement Learning

Doudou Zhou^{1*}, Yufeng Zhang^{2*}, Aaron Sonabend-W³,
Zhaoran Wang², Junwei Lu⁴, Tianxi Cai^{4,5}

¹Department of Statistics, University of California, Davis

²Departments of Industrial Engineering and Management Sciences, Northwestern University
Google Inc.

⁴Department of Biostatistics, Harvard T.H. Chan School of Public Health

⁵Department of Biomedical Informatics, Harvard Medical School

June 14, 2022

Abstract

Evidence-based or data-driven dynamic treatment regimes are essential for personalized medicine, which can benefit from offline reinforcement learning (RL). Although massive healthcare data are available across medical institutions, they are prohibited from sharing due to privacy constraints. Besides, heterogeneity exists in different sites. As a result, federated offline RL algorithms are necessary and promising to deal with the problems. In this paper, we propose a multi-site Markov decision process model which allows both homogeneous and heterogeneous effects across sites. The proposed model makes the analysis of the site-level features possible. We design the first federated policy optimization algorithm for offline RL with sample complexity. The proposed algorithm is communication-efficient and privacy-preserving, which requires only a single round of communication interaction by exchanging summary statistics. We give a theoretical guarantee for the proposed algorithm without the assumption of sufficient action coverage, where the suboptimality for the learned policies is comparable to the rate as if data is not distributed. Extensive simulations demonstrate the effectiveness of the proposed algorithm. The method is applied to a sepsis data set in multiple sites to illustrate its use in clinical settings.

Keywords: dynamic treatment regimes, multi-source learning, electrical health records

*Zhou and Zhang contributed equally

1 Introduction

1.1 Background

The construction of evidence-based or data-driven dynamic treatment regimes (DTRs) (Murphy et al., 2001; Lavori and Dawson, 2004) is a central problem for personalized medicine. Reinforcement learning (RL) models, which often treat the observations by the episodic Markov decision process (MDP) (Puterman, 2014; Sutton and Barto, 2018) have shown remarkable success for these applications. For instance, RL models have been used for deciding optimal treatments and medication dosage in sepsis management (Raghu et al., 2017; Sonabend et al., 2020; Komorowski et al., 2018), HIV therapy selection (Parbhoo et al., 2017), inflammatory bowel disease treatment (Sonabend et al., 2020), and the management of invasive mechanical ventilation (Prasad et al., 2017).

With increasingly available massive healthcare datasets such as the EHR data (Johnson et al., 2016) and mobile health data (Xu et al., 2021), and due to the high risk of direct interventions on patients and the expensive cost of conducting clinical trials (Chakraborty and Murphy, 2014), offline RL is usually preferred for finding DTRs (Murphy, 2003; Robins, 2004; Chakraborty, 2013), whose objective is to learn an optimal policy based on existing datasets (Lange et al., 2012; Levine et al., 2020; Kidambi et al., 2020; Sonabend et al., 2020). For example, the mobile health data are employed for controlling blood glucose levels in patients with type 1 diabetes (Luckett et al., 2020) and the diagnosis of depression (Xu et al., 2021) due to the increasing popularity of mobile devices (Free et al., 2013; Steinhubl et al., 2013).

However, the healthcare data are often distributed in different sites. For instance, the EHR data are always stored locally in different hospitals (Hong et al., 2021) and the

mobile health data are recorded and stored in the users' own mobile devices (Xu et al., 2021). Although the aggregation of multi-site data can improve the quality of the models, for the protection of data privacy (Agu et al., 2013; Cao et al., 2017), different medical institutions are often not allowed to share data (Hao et al., 2019), which hinders the direct aggregation of multi-site data (Hao et al., 2019; Duchi et al., 2014) and affects the model accuracy significantly (Li et al., 2019).

Besides, heterogeneity exists in different sites. For instance, patients are only given some specific drugs in a hospital due to the local suppliers, so models trained on a single site can mislead agents because of the limited actions. Similarly, the doctors in the same hospital may follow a common treatment procedure, which will cause insufficient exploration of the MDP. As a result, the trajectories in a single hospital may have a substantially different distribution from that induced by the optimal policy (or the target policy), which is known as distribution shift (Levine et al., 2020).

1.2 Overview of the Proposed Model and Algorithm

To resolve these challenges, in this paper, we propose a multi-site MDP model which allows heterogeneity among different sites to address previously discussed issues. To be specific, we consider the setting with K sites generated from the episodic linear MDP (Puterman, 2014; Sutton and Barto, 2018) with the state space \mathcal{S} , action space \mathcal{A} and horizon H which will be detailed in Section 2. We incorporate heterogeneity by allowing the transition kernel $\mathcal{P}^k = \{\mathbb{P}_h^k\}_{h=1}^H$ and the reward function $r^k = \{r_h^k\}_{h=1}^H$ to be different for the K sites specified as follows:

$$\mathbb{P}_h^k(x_{h+1} \mid x_h, a_h) = \langle \phi_1(x_h, a_h), \mu_h^k(x_h) \rangle, \quad (1)$$

$$\mathbb{E}[r_h^k(x_h, a_h) \mid x_h, a_h] = \langle \phi_0(x_h, a_h), \theta_h^0 \rangle + \langle \phi_1(x_h, a_h), \theta_h^k \rangle \quad (2)$$

for $k \in [K], h \in [H]$, where x_h and a_h are the state and action in the time h , respectively, μ_h^k 's are unknown measures over \mathcal{S} , and ϕ_0 and ϕ_1 are known feature maps. The feature maps can be thought of the representation for relevant covariates which may vary over time. Here we assume that ϕ_0 is the site-level feature map and ϕ_1 is the individual level feature map. The site-level covariates can contain the type of the hospitals and the number of doctors, while the individual level covariates can contain the demographics, vitals, and lab test results.

The proposed model allows the analysis of site-specific information, which is helpful and sometimes necessary to learn optimal policies for sequential clinical decision-making (Gottesman et al., 2018). For example, the hospital-level information such as the number of intensive care unit (ICU) and the ratio between doctors/nurses and patients is related to the mortality of COVID-19 (Roomi et al., 2021). Another example is the sepsis treatment, where patients are admitted from different sources such as the emergency department, the operating room and the chest pain center. The patients will be also admitted to different types of ICUs according to their infection sites and severity such as cardiac surgery ICU and surgical ICU. It is shown that the optimal treatment rules can be very different for different types of ICU (Zhang et al., 2020).

Since the site-level covariates are usually invariant in the trajectory, it is natural to assume (1) that the transition probability only depends on the individual level covariates and the heterogeneous is incorporated by the site-specific measure μ_h^k . The reward function defined in (2) has two components. The first term is $\langle \phi_0(x, a), \theta_h^0 \rangle$, which is shared by the K sites and dependent on the site-specific features, while the second term is $\langle \phi_1(x, a), \theta_h^k \rangle$, heterogeneous for each site. Under this model, we propose a federated dynamic treatment regime algorithm (FDTR) to estimate the model parameters and learn the optimal policy.

The algorithm consists of two steps. In the first step, the local dynamic treatment regime algorithm (LDTR) adapted from pessimistic variant of the value iteration algorithm (PEVI) (Jin et al., 2021) is run at each site, which learns the optimal policies and the corresponding value functions for each site using its own data only. Pevi incorporates an uncertainty quantifier as the penalty function, thus eliminating the spurious correlation which arises from the trajectories less irrelevant and not informative for the optimal policy. In the second step, the summary statistics involving the learned value functions rather than the individual level data are shared across the sites. By utilizing these summary statistics, each site updates its policy using pessimism again. With the two steps, FDTR achieves efficient communication and preserves privacy by sharing necessary summary statistics only once. The illustration of FDTR workflow is presented in Figure 1.

1.3 Related Work

With data from a single source, offline RL methods, such as Q-learning and the Pevi, have been developed to estimate optimal DTR (Levine et al., 2020; Jin et al., 2021). Existing offline RL methods typically require strong assumptions on the collected data such as sufficient coverage (Fujimoto et al., 2019; Agarwal et al., 2020; Gulcehre et al., 2020), the ratio between the visitation measure of the target policy and behavior policies (Jiang and Li, 2016; Thomas and Brunskill, 2016; Zhang et al., 2020; Sonabend et al., 2020), or a similar ratio over the state-action space (Antos et al., 2008; Liu et al., 2019; Scherrer et al., 2015). However, these assumptions either tend to be violated in healthcare settings or are not verifiable.

One approach to overcome such challenges is to train optimal DTR using data from multiple institutions. To further mitigate data sharing constraints, federated learning methods

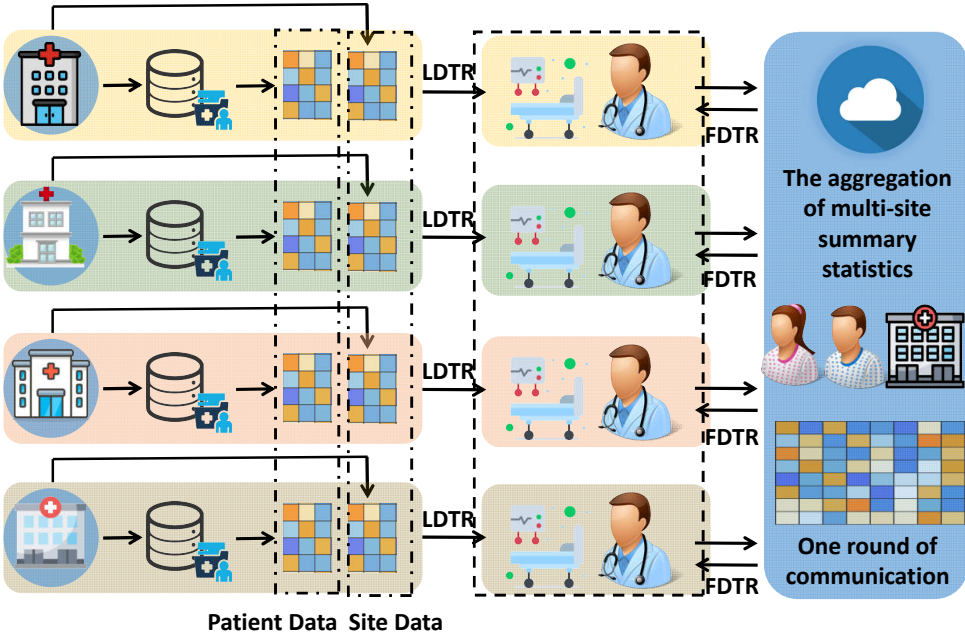


Figure 1: An illustration of FDTR. First, each site (e.g., hospital) trains LDTR using its own data, then uploads both the site-level and patient-level summary statistics to the center. Next, the hospital downloads all hospitals’ summary statistics from the center and utilizes these summary statistics and its data to train FDTR.

have been developed in recent years to enable co-training algorithms based on shared summary level data. Federated learning algorithms have been successfully developed for many tasks including prediction (Min et al., 2019; Hard et al., 2018), classification or clustering (Konečný et al., 2016; McMahan et al., 2017; Yang et al., 2019). Communication-efficient and privacy-preserving algorithms with statistical guarantees have been developed for parametric likelihood framework (Jordan et al., 2019; Battey et al., 2018; Duan et al., 2022; Cai et al., 2021) and the modern machine learning models (Wang et al., 2019; Elgabli et al., 2020).

In recent years, federated RL algorithms have also been proposed to co-train the underlying model overcoming data sharing constraints (Zhuo et al., 2019; Nadiger et al., 2019;

Lim et al., 2020). However, these algorithms focus on the online RL setting which prevents them from being used for finding DTRs, additionally, the most of them lack theoretical guarantees. Federated RL is also different from multi-agent RL (Chen et al., 2018; Zhang et al., 2019), which considers the interaction of several agents in a common environment as illustrated by Zhuo et al. (2019). Limited methods exist for federated offline RL. Under homogeneous settings where the underlying models are assumed to be identical across sites, one may train local DTRs within each site and then obtain a combined estimate by averaging the local DTR estimates across sites. However, such an approach cannot accommodate cross-site heterogeneity. As far as we are aware, no existing methods can perform co-training federated offline RL models in the presence of heterogeneity.

1.4 Our Contributions

To the best of our knowledge, the proposed FDTR is the first federated policy optimization algorithm for offline RL with sample complexity. It allows for both homogeneous and heterogeneous effects across sites with strong theoretical guarantees, and only requires a single round of communication exchange among different sites. More specifically, our paper has the following three contributions. First, we propose a novel multi-site MDP model which incorporates the site-level and individual-level features for clinicians to make adaptive site-dependent treatments. In some cases, the site-level feature ϕ_0 is constant in the same site, under which case the site-specific coefficients can not be estimated by utilizing the single-site data. The proposed model makes the analysis of the site-level features possible. Second, we design an communication-efficient and privacy-preserving algorithm FDTR which requires a single round of communication interaction by exchanging summary statistics. Our approach does not require multiple communications such sharing

evaluated gradient at each step of the DTR training. Third, we give theoretical guarantee for the proposed algorithm without the assumption of sufficient action coverage, a strong assumption which is often violated for clinical trials and observational healthcare data, due to the limited feasible treatments and sample size (Gottesman et al., 2018, 2019). Instead, we assume independence of the trajectories, a weaker assumption that is easier to be satisfied in reality within many disease contexts such as cancer, sepsis, and others. We provide theoretical results for FDTR, which guarantee suboptimality for the learned policies that is comparable to the rate as if data is not distributed. We also control the estimation error of the site-specific coefficients of interest, which can not be estimated using single site data.

1.5 Outline of the Paper

We organize the rest of the paper as follows. In Section 2, we formally introduce the multi-site DTR model. In Section 3, we present the objective functions and the FDTR algorithm. We then show the suboptimality of FDTR in Section 4. Simulations are conducted in Section 5.1 and a real data application is given in Section 5.2.

2 Multi-site MDP Model

2.1 Notation

We use $\|\cdot\|$ as the ℓ_2 -norm for a vector, $\|\cdot\|_{\text{op}}$ as the operator norm of a matrix. For two vectors w and θ with same dimension, we use $\langle w, \theta \rangle$ to denote their inner product $w^\top \theta$. Besides, for any positive integer d , we use $[d]$ to denote the index set $\{1, \dots, d\}$. For a matrix \mathbf{W} , we use \mathbf{W}^+ to denote its Moore-Penrose inverse. We use \mathbf{I}_d to denote the

$d \times d$ identity matrix. For two symmetric matrices \mathbf{A} and \mathbf{B} of the same dimension, we say $\mathbf{A} \geq \mathbf{B}$ if $\mathbf{A} - \mathbf{B}$ is positive semi-definite. For two real numbers $a, b \in \mathbb{R}$, we use $\min\{a, b\}^+$ to denote $\max\{\min\{a, b\}, 0\}$. Besides, we use $a_n = \tilde{O}(b_n)$ to denote a_n is upper bounded by b_n up to some logarithmic factors.

2.2 Model

In this section, we introduce in details about our multi-site MDP model. Given the k th site for $k \in [K]$, a dataset $\mathcal{D}_k = \{(x_h^{k,\tau}, a_h^{k,\tau}, r_h^{k,\tau})\}_{\tau,h=1}^{n_k, H}$ is collected a priori where at each step $h \in [H]$ of each trajectory (e.g., patient) $\tau \in [n_k]$, the experimenter (e.g., clinician) takes the action $a_h^{k,\tau} \sim \pi_h^k(a|x_h^{k,\tau})$ at the state $x_h^{k,\tau}$, receives the reward $r_h^{k,\tau} = r_h^k(x_h^{k,\tau}, a_h^{k,\tau})$ satisfying (2), and observes the next state $x_{h+1}^{k,\tau} \sim \mathbb{P}_h^k(\cdot \mid x_h = x_h^{k,\tau}, a_h = a_h^{k,\tau})$ satisfying (1). The feature maps $\phi_0(x, a) \in \mathbb{R}^{d_0}$ and $\phi_1(x, a) \in \mathbb{R}^{d_1}$ in (1) and (2) are pre-specified. In order to guarantee sample complexity and model identifiability, we assume no co-linearity between $\phi_0(x, a)$ and $\phi_1(x, a)$ ¹. The transition probabilities only depend on features specified in $\phi_1(x, a)$ and we let $\phi_0(x, a)$ include site-level features and features with effects that are common across sites. For example, we can allow the age categories (e.g., children or adults) to have common effect across sites, which are contained by ϕ_0 , while allowing for a small degree of heterogeneity by including linear age effects in ϕ_1 . All trajectories in \mathcal{D}_k are assumed to be independent and the K sites are also independent. We do not impose any constraint on the behavior policies π_h^k 's, which are allowed to be different in the K sites.

¹See in details in Remark 5.

2.3 Bellman Equation

For any policy $\pi = \{\pi_h\}_{h=1}^H$, we define the (state-)value function $V_h^{k,\pi} : \mathcal{S} \rightarrow \mathbb{R}$ for the k th site at each step $h \in [H]$ as

$$V_h^{k,\pi}(x) = \mathbb{E}_{k,\pi} \left[\sum_{t=h}^H r_t^k(x_t, a_t) \mid x_h = x \right] \quad (3)$$

and the action-value function (Q-function) $Q_h^{k,\pi} : \mathcal{S} \times \mathcal{A} \rightarrow \mathbb{R}$ at each step $h \in [H]$ as

$$Q_h^{k,\pi}(x, a) = \mathbb{E}_{k,\pi} \left[\sum_{t=h}^H r_t^k(x_t, a_t) \mid x_h = x, a_h = a \right]. \quad (4)$$

Here the expectation $\mathbb{E}_{k,\pi}$ in (3) and (4) is taken with respect to the randomness of the trajectory induced by π , which is obtained by taking the action $a_t \sim \pi_t(\cdot \mid x_t)$ at the state x_t and observing the next state $x_{t+1} \sim \mathbb{P}_t^k(\cdot \mid x_t, a_t)$ at each step $t \in [H]$. Meanwhile, we fix $x_h = x \in \mathcal{S}$ in (3) and $(x_h, a_h) = (x, a) \in \mathcal{S} \times \mathcal{A}$ in (4). By the Bellman equation, we have

$$V_h^{k,\pi}(x) = \langle Q_h^{k,\pi}(x, \cdot), \pi_h(\cdot \mid x) \rangle_{\mathcal{A}},$$

$$Q_h^{k,\pi}(x, a) = \mathbb{E}_k [r_h^k(x_h, a_h) + V_{h+1}^{k,\pi}(x_{h+1}) \mid x_h = x, a_h = a],$$

where $\langle \cdot, \cdot \rangle_{\mathcal{A}}$ is the inner product over \mathcal{A} , while \mathbb{E}_k is taken with respect to the randomness of the immediate reward $r_h^k(x_h, a_h)$ and next state x_{h+1} where $x_{h+1} \sim \mathbb{P}_h^k(x_{h+1} \mid x_h, a_h)$. For the k th hospital and any function $f : \mathcal{S} \rightarrow \mathbb{R}$, we define the transition operator at each step $h \in [H]$ as

$$(\mathbb{P}_h^k f)(x, a) = \mathbb{E}_k [f(x_{h+1}) \mid x_h = x, a_h = a]$$

and the Bellman operator at each step $h \in [H]$ as

$$\begin{aligned} (\mathbb{B}_h^k f)(x, a) &= \mathbb{E}_k [r_h^k(x_h, a_h) + f(x_{h+1}) \mid x_h = x, a_h = a] \\ &= \mathbb{E}_k [r_h^k(x_h, a_h) \mid x_h = x, a_h = a] + (\mathbb{P}_h^k f)(x, a). \end{aligned} \quad (5)$$

As a result, by (1) and (2), for any function V , there exists $\bar{\theta}_h^k \in \mathbb{R}^{d_1}$ such that

$$(\mathbb{B}_h^k V)(x, a) = \langle \phi_0(x, a), \theta_h^0 \rangle + \langle \phi_1(x, a), \bar{\theta}_h^k \rangle, \quad (6)$$

where $\bar{\theta}_h^k = \theta_h^k + \int_{x' \in \mathcal{S}} \mu_h^k(x') V(x') dx'$. Therefore, the coefficients θ_h^0 and $\bar{\theta}_h^k$ can be estimated through linear regression if the values $(\mathbb{B}_h^k V)(x, a)$ are known, which inspires us to derive the FDTR algorithm.

3 Federated Dynamic Treatment Regimes Algorithm

Suppose that we are treating the k th site. Inspired by (6), we notice the key step is to construct estimates \hat{V}_h^k of V_h^k and $\hat{\mathbb{B}}_h^k \hat{V}_{h+1}^k$ of $\mathbb{B}_h^k V_h^k$ based on \mathcal{D}_k and the summary statistics of $\{\mathcal{D}_j\}_{j \neq k}$. As mentioned in the Section 1, the pessimism plays an important role in the control of suboptimality. Define $\mathcal{D} = \cup_{k=1}^K \mathcal{D}_k$. Following the line of Jin et al. (2021), we achieve pessimism by the notion of multi-site confidence bound Γ_h^k with the confidence parameter $\xi \in (0, 1)$ as follows.

Definition 1 (Multi-site confidence bound) *For the k th site, we say $\{\Gamma_h^k : \mathcal{S} \times \mathcal{A} \rightarrow \mathbb{R}\}_{h=1}^H$ is a ξ -multi-site confidence bound of $V = \{V_h\}_{h=1}^H$ with respect to $\mathbb{P}_{\mathcal{D}}$ if the event*

$$\mathcal{E}_k(V) = \left\{ |(\hat{\mathbb{B}}_h^k V_{h+1})(x, a) - (\mathbb{B}_h^k V_{h+1})(x, a)| \leq \Gamma_h^k(x, a) \text{ for all } (x, a) \in \mathcal{S} \times \mathcal{A}, h \in [H] \right\} \quad (7)$$

satisfies $\mathbb{P}_{\mathcal{D}}(\mathcal{E}_k(V)) \geq 1 - \xi$. Here the value functions $V = \{V_h\}_{h=1}^H$ and $\{\Gamma_h^k\}_{h=1}^H$ can depend on \mathcal{D} . Specifically, if both of them only depend on \mathcal{D}_k , then $\mathbb{P}_{\mathcal{D}}(\mathcal{E}_k(V)) = \mathbb{P}_{\mathcal{D}_k}(\mathcal{E}_k(V))$.

By the definition, Γ_h^k quantifies the approximation error of $\hat{\mathbb{B}}_h^k V_{h+1}$ for $\mathbb{B}_h^k V_{h+1}$, which plays an important role in eliminating the spurious correlation as discussed by Jin et al. (2021).

Before we present the detail of the FDTR algorithm, we introduce the following notations

for simplicity:

$$\begin{aligned}
\Phi_{0,h}^k &= (\phi_0(x_h^{k,1}, a_h^{k,1}), \dots, \phi_0(x_h^{k,n_k}, a_h^{k,n_k}))^\top; \Phi_{1,h}^k = (\phi_1(x_h^{k,1}, a_h^{k,1}), \dots, \phi_1(x_h^{k,n_k}, a_h^{k,n_k}))^\top; \\
\Phi_h^k &= (\phi^k(x_h^{k,1}, a_h^{k,1}), \dots, \phi^k(x_h^{k,n_k}, a_h^{k,n_k}))^\top; \Phi_h = ((\Phi_h^1)^\top, \dots, (\Phi_h^K)^\top); \Lambda_h = \Phi_h^\top \Phi_h; \\
\mathbf{Y}_h^k(V) &= (r_h^{k,1} + V(x_{h+1}^{k,1}), \dots, r_h^{k,n_k} + V(x_{h+1}^{k,n_k}))^\top; \Lambda_h^k = (\Phi_{0,h}^k, \Phi_{1,h}^k)^\top (\Phi_{0,h}^k, \Phi_{1,h}^k);
\end{aligned} \tag{8}$$

where $\phi^k(x, a) = (\phi_0(x, a)^\top, \mathbf{0}_{(j-1)d_1}^\top, \phi_1(x, a)^\top, \mathbf{0}_{(K-j)d_1}^\top)^\top \in \mathbb{R}^{d_K}$ with $d_K = d_0 + d_1 K$, and $V : \mathcal{S} \rightarrow \mathbb{R}$ is some value function. Besides, let $\phi(x, a) = (\phi_0(x, a)^\top, \phi_1(x, a)^\top)^\top \in \mathbb{R}^d$ where $d = d_0 + d_1$ and $N = \sum_{k=1}^K n_k$. We define the empirical mean squared Bellman error (MSBE):

$$M_h^k(\boldsymbol{\beta}^0, \boldsymbol{\beta}^k \mid \widehat{V}_{h+1}^k, \mathcal{D}_k) = \|\mathbf{Y}_h^k(\widehat{V}_{h+1}^k) - \Phi_{0,h}^k \boldsymbol{\beta}_0 - \Phi_{1,h}^k \boldsymbol{\beta}_k\|^2 \text{ for } h \in [H], k \in [K]. \tag{9}$$

If the patient-level information is shareable across the K hospitals, we can aggregate $M_h^k(\boldsymbol{\beta}_0, \boldsymbol{\beta}_k \mid \widehat{V}_{h+1}^k, \mathcal{D}_k)$ for $k \in [K]$ to estimate $\boldsymbol{\beta}_0$ and $\boldsymbol{\beta}_k$ for $k \in [K]$ simultaneously. However, as we state above, it is usually not possible in reality due to privacy concern. On the contrary, we assume that we have some preliminary estimators for the value functions $\{\widetilde{V}_h^k\}_{k,h=1}^{K,H}$. Here we adopt the PEVI of linear MDP algorithm in [Jin et al. \(2021\)](#) to obtain the preliminary estimators $\{\widetilde{V}_h^k\}_{k,h=1}^{K,H}$, which is summarized in Algorithm 1. We consider the objective function for $\boldsymbol{\beta} = ((\boldsymbol{\beta}^0)^\top, (\boldsymbol{\beta}^1)^\top, \dots, (\boldsymbol{\beta}^K)^\top)^\top \in \mathbb{R}^{d_K}$:

$$\begin{aligned}
f(\boldsymbol{\beta} \mid \widehat{V}_{h+1}^k, \{\widetilde{V}_{h+1}^j\}_{j \in [K], j \neq k}, \mathcal{D}) &= \sum_{j \neq k}^K M_h^j(\boldsymbol{\beta}^0, \boldsymbol{\beta}^j \mid \widetilde{V}_{h+1}^j, \mathcal{D}_j) \\
&\quad + M_h^k(\boldsymbol{\beta}^0, \boldsymbol{\beta}^k \mid \widehat{V}_{h+1}^k, \mathcal{D}_k) + \lambda(\|\boldsymbol{\beta}_0\|^2 + \|\boldsymbol{\beta}_k\|^2),
\end{aligned} \tag{10}$$

which has the explicit solution

$$\begin{aligned}
\widehat{\boldsymbol{\beta}}_h &= ((\widehat{\boldsymbol{\beta}}_h^0)^\top, \dots, (\widehat{\boldsymbol{\beta}}_h^K)^\top)^\top = \arg \min_{\boldsymbol{\beta} \in \mathbb{R}^{d_K}} f(\boldsymbol{\beta} \mid \widehat{V}_{h+1}^k, \{\widetilde{V}_{h+1}^j\}, \mathcal{D}) \\
&= (\Lambda_h + \mathbf{H}_\lambda)^+ \left\{ \sum_{j \neq k}^K (\Phi_h^j)^\top \mathbf{Y}_h^j (\widetilde{V}_{h+1}^j) + (\Phi_h^k)^\top \mathbf{Y}_h^k (\widehat{V}_{h+1}^k) \right\},
\end{aligned} \tag{11}$$

Algorithm 1 Local Dynamic Treatment Regime (LDTR).

- 1: **for** site $k = 1, 2, \dots, K$ **do**
- 2: Input: Dataset $\mathcal{D} = \{(x_h^{k,\tau}, a_h^{k,\tau}, r_h^{k,\tau})\}_{\tau,h=1}^{n_k, H}$.
- 3: Set $\lambda = 1$, $\alpha_k = cdH\sqrt{\zeta_k}$, where $\zeta_k = \log(2dHn_k/\xi)$.
- 4: Initialization: set $\tilde{V}_{H+1}^k(x) \leftarrow 0$.
- 5: **for** step $h = H, H-1, \dots, 1$ **do**
- 6: Set Λ_h^k as in (8).
- 7: Set $\tilde{\beta}_h^k = (\Lambda_h^k + \lambda \mathbf{I}_d)^{-1} (Y_h^k (\tilde{V}_{h+1}^k)^\top \Phi_{0,h}^k, Y_h^k (\tilde{V}_{h+1}^k)^\top \Phi_{1,h}^k)^\top$.
- 8: Set $\tilde{\Gamma}_h^k(\cdot, \cdot) \leftarrow \alpha_k (\phi(\cdot, \cdot)^\top (\Lambda_h^k + \lambda \mathbf{I}_d)^{-1} \phi(\cdot, \cdot))^{1/2}$.
- 9: Set $\tilde{Q}_h^k(x, a) \leftarrow \min \{\phi(x, a)^\top \tilde{\beta}_h^k - \tilde{\Gamma}_h^k(x, a), H-h+1\}^+$.
- 10: Set $\tilde{\pi}_h^k(\cdot | \cdot) \leftarrow \arg \max_{\pi_h} \langle \tilde{Q}_h^k(\cdot, \cdot), \pi_h(\cdot | \cdot) \rangle_{\mathcal{A}}$.
- 11: Set $\tilde{V}_h^k(\cdot) \leftarrow \langle \tilde{Q}_h^k(\cdot, \cdot), \tilde{\pi}_h^k(\cdot | \cdot) \rangle_{\mathcal{A}}$.
- 12: Output: $\tilde{\pi}^k = \{\tilde{\pi}_h^k\}_{h=1}^H$, $\tilde{V}^k = \{\tilde{V}_h^k\}_{h=1}^H$.

where $\mathbf{H}_\lambda = \text{diag}(\lambda \mathbf{1}_{d_0}, \mathbf{0}_{d_1(k-1)}, \lambda \mathbf{1}_{d_1}, \mathbf{0}_{d_1(K-k)})$. Define

$$\Sigma_h^k = \Lambda_h^k + \lambda I_d + \begin{bmatrix} \sum_{j \neq k}^K (\Phi_{0,h}^j)^\top (\mathbf{I}_{n_j} - \mathbf{P}_{\Phi_{1,h}^j}) \Phi_{0,h}^j & \mathbf{0}_{d_0 \times d_1} \\ \mathbf{0}_{d_1 \times d_0} & \mathbf{0}_{d_1 \times d_1} \end{bmatrix} \in \mathbb{R}^{d \times d}, \quad (12)$$

where $\mathbf{P}_{\Phi_{1,h}^j} = \Phi_{1,h}^j ((\Phi_{1,h}^j)^\top \Phi_{1,h}^j)^+ (\Phi_{1,h}^j)^\top \in \mathbb{R}^{n_j \times n_j}$ is the projection matrix to the column space of $\Phi_{1,h}^j$. Correspondingly, we set

$$(\widehat{\mathbb{B}}_h^k \widehat{V}_{h+1}^k)(x, a) = \phi^k(x, a)^\top \widehat{\beta}_h^k = \phi_0(x, a)^\top \widehat{\beta}_h^0 + \phi_1(x, a)^\top \widehat{\beta}_h^k.$$

Meanwhile, we construct Γ_h^k based on \mathcal{D} as

$$\widehat{\Gamma}_h^k(x, a) = \alpha (\phi^k(x, a)^\top (\Lambda_h + \mathbf{H}_\lambda)^{-1} \phi^k(x, a))^{1/2} = \alpha (\phi(x, a)^\top (\Sigma_h^k)^{-1} \phi(x, a))^{1/2} \quad (13)$$

at each step $h \in [H]$, where the second equality comes from the block-wise formula of the matrix inverse. Here $\alpha > 0$ is the scaling parameter. In addition, we construct \widehat{V}_h^k based

Algorithm 2 Federated Dynamic Treatment Regime (FDTR): the update for the k th site.

- 1: Input: Dataset $\mathcal{D}_k = \{(x_h^{k,\tau}, a_h^{k,\tau}, r_h^{k,\tau})\}_{\tau,h=1}^{n_k, H}$. The summary statistics from the other $K - 1$ sites
$$\{(\Phi_h^j)^\top \Phi_h^j, (\Phi_h^j)^\top \mathbf{Y}_h^j (\tilde{V}_{h+1}^j)\}_{h=1}^H, \text{ for } j \in [K], j \neq k.$$
- 2: Set $\lambda = 1$, $\alpha = cdH\sqrt{\zeta}$, where $\zeta = \log(2dHN/\xi)$.
- 3: Initialization: set $\hat{V}_{H+1}^k(x) \leftarrow 0$.
- 4: **for** step $h = H, H - 1, \dots, 1$ **do**
- 5: Set $\hat{\beta}_h$ as in (11) and $\hat{\Gamma}_h^k(\cdot, \cdot)$ as in (13).
- 6: Set $\hat{Q}_h^k(\cdot, \cdot) \leftarrow \min \{\phi^k(\cdot, \cdot)^\top \hat{\beta}_h - \hat{\Gamma}_h^k(\cdot, \cdot), H - h + 1\}^+$.
- 7: Set $\hat{\pi}_h^k(\cdot | \cdot) \leftarrow \arg \max_{\pi_h} \langle \hat{Q}_h^k(\cdot, \cdot), \pi_h(\cdot | \cdot) \rangle_{\mathcal{A}}$.
- 8: Set $\hat{V}_h^k(\cdot) \leftarrow \langle \hat{Q}_h^k(\cdot, \cdot), \hat{\pi}_h^k(\cdot | \cdot) \rangle_{\mathcal{A}}$.
- 9: Output: $\hat{\pi}^k = \{\hat{\pi}_h^k\}_{h=1}^H$.

on \mathcal{D} as

$$\begin{aligned} \hat{Q}_h^k(x, a) &= \min\{\bar{Q}_h^k(x, a), H - h + 1\}^+, \quad \text{where } \bar{Q}_h^k(x, a) = (\hat{\mathbb{B}}_h^k \hat{V}_{h+1}^k)(x, a) - \hat{\Gamma}_h^k(x, a), \\ \hat{V}_h^k(x) &= \langle \hat{Q}_h^k(x, \cdot), \hat{\pi}_h^k(\cdot | x) \rangle_{\mathcal{A}}, \quad \text{where } \hat{\pi}_h^k(\cdot | x) = \arg \max_{\pi_h} \langle \hat{Q}_h^k(x, \cdot), \pi_h(\cdot | x) \rangle_{\mathcal{A}}. \end{aligned}$$

Notice that the above procedures only require summary statistics from other sites. To be specific, only $(\Phi_h^j)^\top \Phi_h^j$ and $(\Phi_h^j)^\top \mathbf{Y}_h^j (\tilde{V}_{h+1}^j)$, for $j \in [K], j \neq k$ are required when we are treating the k th site. The FDTR is summarized in Algorithm 2. The communication cost is $O(Kd^2)$ for sharing the summary statistics and the computational complexity is $O(HdN + KHd^3)$ for calculating the summary statistics and conducting KH linear regressions.

4 Theoretical Analysis

In this section, we state the theoretical properties of FDTR. For the multi-site MDP $(\mathcal{S}, \mathcal{A}, H, \mathcal{P}^k, r^k)$, we use $\pi^{k,*}$, $Q_h^{k,*}$, and $V_h^{k,*}$ to denote the optimal policy, optimal Q-function, and optimal value function for the k th site, respectively. We have $V_{H+1}^{k,*} = 0$ and the Bellman optimality equation

$$V_h^{k,*}(x) = \max_{a \in \mathcal{A}} Q_h^{k,*}(x, a), \quad Q_h^{k,*}(x, a) = (\mathbb{B}_h^k V_{h+1}^{k,*})(x, a).$$

Meanwhile, the optimal policy $\pi^{k,*}$ is specified by

$$\pi_h^{k,*}(\cdot | x) = \arg \max_{\pi_h} \langle Q_h^{k,*}(x, \cdot), \pi_h(\cdot | x) \rangle_{\mathcal{A}}, \quad V_h^{k,*}(x) = \langle Q_h^{k,*}(x, \cdot), \pi_h^{k,*}(\cdot | x) \rangle_{\mathcal{A}},$$

where the maximum is taken over all functions mapping from \mathcal{S} to distributions over \mathcal{A} . We aim to learn a policy that maximizes the expected cumulative reward. Correspondingly, we define the performance metric at the k th site as

$$\text{SubOpt}^k(\pi; x) = V_1^{\pi^{k,*}}(x) - V_1^{\pi}(x), \quad (14)$$

which is the suboptimality of the policy π given the initial state $x_1 = x$.

We are presenting both data-dependent and explicit rate results. The data-dependent results are more adaptive to the concrete realization of the data and require less assumptions, while the explicit rate results are more straightforward and easier to compare, and give more insights on how the suboptimality and the parameter rate depend on the sample size n_k , the feature dimension d and the number of sites K . For technical simplicity, we assume that $\|\phi_0(x, a)\|^2 + \|\phi_1(x, a)\|^2 \leq 1$ for all $(x, a) \in \mathcal{S} \times \mathcal{A}$, $\|\theta_h^0\| \leq \sqrt{d_0}$, $\max_{k \in [K], h \in [H]} \{\|\mu_h^k(\mathcal{S})\|, \|\theta_h^k\|\} \leq \sqrt{d_1}$, which can be guaranteed after suitable normalization, where with an abuse of notation, we define $\|\mu_h^k(\mathcal{S})\| = \int_{\mathcal{S}} \|\mu_h^k(x)\| dx$. Theorems 1 and 2 characterize the data-dependent suboptimality of Algorithms 1 and 2, respectively.

Theorem 1 (Suboptimality of the Preliminary Estimators) *In Algorithm 1, we set*

$$\lambda = 1, \quad \alpha_k = cdH\sqrt{\zeta_k}, \quad \text{where } \zeta_k = \log(2dHn_k/\xi).$$

Here $c > 0$ is an absolute constant and $\xi \in (0, 1)$ is the confidence parameter. The following statements hold:

1. $\{\tilde{\Gamma}_h^k\}_{h=1}^H$ in Algorithm 1 is a ξ -multi-site confidence bound of $\tilde{V}^k = \{\tilde{V}_h^k\}_{h=1}^H$.
2. For any $x \in \mathcal{S}$, $\tilde{\pi}^k = \{\tilde{\pi}_h^k\}_{h=1}^H$ in Algorithm 1 satisfies

$$\text{SubOpt}^k(\tilde{\pi}_1^k; x) \leq 2\alpha_k \sum_{h=1}^H \mathbb{E}_{k, \pi^{k,*}} \left[\left(\phi(x_h, a_h)^\top (\Lambda_h^k + \lambda I_d)^{-1} \phi(x_h, a_h) \right)^{1/2} \mid x_1 = x \right]. \quad (15)$$

with probability at least $1 - \xi$, for any $k \in [K]$.

Here $\mathbb{E}_{k, \pi^{k,*}}$ is taken with respect to the trajectory induced by $\pi^{k,*}$ in the underlying MDP given the fixed matrix Λ_h^k .

Theorem 1 only uses the local data and the suboptimality does not have an explicit upper bound only depending on the sample size and dimension. Below we present the rate of FDTR as a comparison and show how our aggregation improves the rate.

Theorem 2 (Suboptimality of FDTR) *In Algorithm 2, we set*

$$\lambda = 1, \quad \alpha = cdH\sqrt{\zeta}, \quad \text{where } \zeta = \log(2dHN/\xi). \quad (16)$$

Here $c > 0$ is an absolute constant and $\xi \in (0, 1)$ is the confidence parameter. The following statements hold:

1. $\{\hat{\Gamma}_h^k\}_{h=1}^H$ in Algorithm 2, which is specified in (13), is a ξ -multi-site confidence bound of $\hat{V}^k = \{\hat{V}_h^k\}_{h=1}^H$ in Algorithm 2.

2. For any $x \in \mathcal{S}$, $\widehat{\pi}^k = \{\widehat{\pi}_h^k\}_{h=1}^H$ in Algorithm 2 satisfies

$$\text{SubOpt}^k(\widehat{\pi}^k; x) \leq 2\alpha \sum_{h=1}^H \mathbb{E}_{k, \pi^{k,*}} \left[(\phi(x_h, a_h)^\top (\Sigma_h^k)^{-1} \phi(x_h, a_h))^{1/2} \mid x_1 = x \right] \quad (17)$$

with probability at least $1 - \xi$, for any $k \in [K]$.

Here $\mathbb{E}_{k, \pi^{k,*}}$ is taken concerning the trajectory induced by $\pi^{k,*}$ in the underlying MDP given the fixed matrix Σ_h^k .

By the definition of Σ_h^k in (12), it is easy to show that $\Sigma_h^k \succeq \Lambda_h^k + \lambda \mathbf{I}_d$, which implies that

$$\phi(x_h, a_h)^\top (\Sigma_h^k)^{-1} \phi(x_h, a_h) \leq \phi(x_h, a_h)^\top (\Lambda_h^k + \lambda \mathbf{I}_d)^{-1} \phi(x_h, a_h).$$

Comparing Theorem 1 and Theorem 2, the scaling parameters β and β_k only have a difference in the log term, while the Theorem 2 has a sharper bound for the expectation term, which is owing to the utilization of multi-site information. We now present the estimation error of θ_h^0 .

Theorem 3 (Estimation error of site-specific coefficients) For β specified in Theorem 2, $\widehat{\beta}_h^0$ estimated in Algorithm 1 satisfies

$$\|\widehat{\beta}_h^0 - \theta_h^0\| \leq \alpha \|(\Sigma_h^k)^{-1}\|_{\text{op}}^{1/2}. \quad (18)$$

with probability at least $1 - \xi$, for any $k \in [K]$.

Recall that θ_h^0 is not estimable when $\phi_0(x, a)$ is a constant vector for the trajectories in same site, since $(\Phi_{0,h}^k)^\top \Phi_{0,h}^k = n_k \phi_0(x_h^{k,\tau}, a_h^{k,\tau}) \phi_0(x_h^{k,\tau}, a_h^{k,\tau})^\top$ for $\tau \in [n_k]$ is a rank-one matrix. However, when we combine K sites, if $K \geq d_0$, under mild conditions, $\sum_{k=1}^K (\Phi_{0,h}^k)^\top \Phi_{0,h}^k$ will be a full rank matrix and θ_h^0 can be estimated with theoretical guarantee, which will be detailed latter.

The above theorems are data-dependent. To present the explicit rates related to the sample sizes $n_k, k \in [K]$, we need to impose more assumptions on the data generation

mechanism. For notational simplicity, we define the following (uncentered) covariance matrices

$$\mathcal{C}_{ij,h}^k = \mathbb{E}_{\mathcal{D}_k} [\phi_i(x_h, a_h) \phi_j(x_h, a_h) \mid x_1 = x] \text{ and } \mathcal{C}_h^k = \mathbb{E}_{\mathcal{D}_k} [\phi(x_h, a_h) \phi(x_h, a_h) \mid x_1 = x], \quad (19)$$

for $i, j = 0, 1$, $h \in [H]$, and $k \in [K]$. By definition, $\mathcal{C}_{00,h}^k$ is the covariance of site-level covariates, $\mathcal{C}_{11,h}^k$ is the covariance of patient level covariates and \mathcal{C}_h^k is their joint covariance matrix. In what follows, we illustrate the necessity of FDTR by considering the setting where the data collecting process well explores the state-action space. Recall that $N = \sum_{k=1}^K n_k$ is the number of trajectories of all the sites. We have the following corollary.

Corollary 4 (Suboptimality of FDTR with Well-Explored Dataset) *Assume that there exists an absolute constant $b > 0$ such that $\mathcal{C}_h^k \geq b\mathbf{I}_d$ for any $h \in [H]$ and $k \in [K]$ and $\|\phi_0(x, a)\|^2 \leq d_0/d$ and $\|\phi_1(x, a)\|^2 \leq d_1/d$. If we choose the tuning parameters as (16), it holds that*

$$\text{SubOpt}^k(\hat{\pi}^k; x) \leq 2\sqrt{2}\alpha H \sqrt{\frac{1}{bd} \left(\frac{d_0}{N} + \frac{d_1}{n_k} \right)} \quad \text{and} \quad \|\hat{\beta}_h^0 - \theta_h^0\| \leq \frac{\sqrt{2}\alpha}{\sqrt{Nb}}$$

with probability at least $1 - 2\xi$.

Remark 5 Notice that $\|\phi_0(x, a)\|^2 + \|\phi_1(x, a)\|^2 \leq 1$. The additional assumption that $\|\phi_0(x, a)\|^2 \leq d_0/d$ and $\|\phi_1(x, a)\|^2 \leq d_1/d$ implies that norm is uniformly distributed among ϕ_0 and ϕ_1 , which is only needed to obtain the explicit rate dependent on d_0, d_1 and d . Otherwise, the upper bound of $\text{SubOpt}^k(\hat{\pi}^k; x)$ can be replaced by

$$2\sqrt{2}\alpha H \sqrt{\|\phi_0(x, a)\|^2 / (\|\phi(x, a)\|^2 bN) + \|\phi_1(x, a)\|^2 / (\|\phi(x, a)\|^2 b n_k)}.$$

Besides, the assumption that $\mathcal{C}_n^k \geq b\mathbf{I}_d$ implies that $\phi_0(x, a)$ and $\phi_1(x, a)$ can not be fully linear dependent, that is, a feature exists in both ϕ_0 and ϕ_1 . Otherwise, \mathcal{C}_n^k may not be full rank, violating the lower bounded eigenvalue assumption. However, the features in ϕ_0 and ϕ_1 can be correlated, as the age covariate example in Section 2.2.

The assumption that $\mathcal{C}_h^k \geq b\mathbf{I}_d$ assumes that the dataset well explores the state and action space (Duan et al., 2020; Jin et al., 2021) in the sense that each direction in the feature space is well explored in the dataset \mathcal{D}_k . When considering the well-explored dataset, Corollary 4 shows that FDTR attains the suboptimality of order $\tilde{O}(H^2d\sqrt{d_0/(dN)} + d_1/(dn_k))$, while the suboptimality of the preliminary estimator is $\tilde{O}(H^2d/\sqrt{n_k})$ (Jin et al., 2021). Thus, FDTR is more efficient than LDTR in eliminating the suboptimality arisen from the site-level features. Specifically, when the total number of trajectories N is much larger than the number of trajectory n_k at site k , FDTR attains the suboptimality of order $\tilde{O}(H^2d\sqrt{d_1/(dn_k)})$, which does not involve the dimension d_0 of the site-level feature. Besides, the statistical rate of $\hat{\beta}_h^0$ is $\tilde{O}(HdN^{-1/2})$. When H and d are fixed, it achieves the standard parametric rate $O(N^{-1/2})$ which performs like pooling all data together.

However, the assumption that $\mathcal{C}_h^k \geq b\mathbf{I}_d$ will be violated when $\text{rank}(\mathcal{C}_{00,h}^k) < d_0$, which happens when $d_0 > 1$ and ϕ_0 is constant in the same site. To this end, θ_h^0 cannot be estimated by using the single site data only. However, θ_h^0 can still be estimated by FDTR as shown by the following corollary. For simplicity, we assume that $n = n_1 = \dots = n_K$.

Corollary 6 (Suboptimality of FDTR with Site-constant Covariates) *We assume that there exists an absolute constant $b > 0$ such that $\mathcal{C}_{11,h}^k \geq b\mathbf{I}_{d_1}$ and*

$$\lambda_{\min}\left(\frac{1}{K} \sum_{k=1}^K \mathcal{C}_{00,h}^k\right) \geq \max\{b, 2b^{-1} \cdot \|\mathcal{C}_{10,h}^k\|^2\} \text{ for all } k \in [K], \quad (20)$$

and $k \in [K]$ and $\|\phi_0(x, a)\|^2 \leq d_0/d$ and $\|\phi_1(x, a)\|^2 \leq d_1/d$. If we choose the tuning parameters as (16), it holds that

$$\text{SubOpt}^k(\hat{\pi}^k; x) \leq 2\sqrt{2}\alpha H \sqrt{\frac{1}{bd} \left(\frac{d_0}{N} + \frac{d_1}{n_k} \right)} \quad \text{and} \quad \|\hat{\beta}_h^0 - \theta_h^0\| \leq \frac{\sqrt{2}\alpha}{\sqrt{Nb}}$$

with probability at least $1 - 2\xi$.

By imposing the assumption in (20), we get the same suboptimality and statistical rate as in Corollary 4. In particular, the assumption in (20) allows for $\text{rank}(\mathcal{C}_{00,h}^k) < d_0$ for a single site k , which allows ϕ_0 to be constant within each site. Recall that \mathcal{C}_h^k is the (uncentered) covariance between the site-level feature ϕ_0 and the individual level feature ϕ_1 . The inequality in (20) holds when such a correlation is relatively small. Besides, we require $\lambda_{\min}(K^{-1} \sum_{k=1}^K \mathcal{C}_{00,h}^k)$ to be relatively large, which holds when the space of site-level features is well-explored by the dataset \mathcal{D} .

5 Experiments

We perform extensive simulations to evaluate the performance of FDTR. In particular, we focus on how well the proposed methods work as we vary the dimension and cardinality of the state and action space, respectively, episode length, and the number of hospitals.

5.1 Simulations

We simulate the data according to the following random MDP. We generate random vectors $\theta_h^0 \in \mathbb{R}^{d_0}$, $\theta_h^k \in \mathbb{R}^{d_1}$ for $k \in [K]$, and matrix $\theta^\mu \in \mathbb{R}^{d_1 \times H}$ where every element follows a $\text{Uniform}(0, 1)$ distribution, which are then normalized to satisfy the assumptions in Section 4. We generate rewards using a Gaussian distribution centered at $\langle \phi_0(x, a), \theta_h^0 \rangle + \langle \phi_1(x, a), \theta_h^k \rangle$ according to (2). Importance sampling is used to sample states from the state transitions density: given state action pair (x, a) we draw the next state from a proposal distribution: $x' \sim q(\cdot | x, a)$ and re-weigh samples using $\mathbb{P}_h^k(x' | x, a) / q(\cdot | x, a)$ with $\mathbb{P}_h^k(x' | x, a) = \langle \phi_1(x, a), \mu_h^k(x') \rangle$, and we use column h in θ^μ as μ_h^k . We clip state vectors and normalize rewards such that $x_h^{k,\tau} \in \mathcal{S}$, $r_h^{k,\tau} \in [0, 1]$ for all $h \in [H]$, $k \in [K]$, $\tau \in [n]$. Finally, we use linear functions with an action-interaction term to represent treatment effect for ϕ_0 ,

ϕ_1 , for example, $\phi_1(x, a) = (x, ax)$.

Hyper-parameters for FDTR training are chosen using 5-fold cross-validation with simulated data, final parameters are set to $\lambda = 1$, $c = .005$, and $\xi = .99$. We implement different benchmark methods to compare the performance of FDTR. The first one is a local DTR (LDTR), which consists of learning a local DTR policy using data from a single hospital site. This LDTR policy can be learned using Algorithm 1 in the Appendix, for a fixed k^* , which yields a policy $\tilde{\pi}^{k^*} = \{\tilde{\pi}_h^{k^*}\}_{h=1}^H$. We then use the K locally trained LDTRs to define LDTR (MV), which given a state, uses majority voting across the K policies to select an action. We also train a Q -learning policy in a single hospital site. We use ordinary least squares to estimate the Q -functions, as these are linear on $\phi(x, a)$. There are three variations of this method. The first, Q -learn (1) uses a single Q -function for any time-step h trained locally in each site. The second selects the most popular action among the K locally trained Q functions; we call this Q -learn (1-MV). The third one, Q -learn (H), is also locally trained Q -learning; however, this one uses a different function $Q_h(\cdot, \cdot)$ for each of the H time steps.

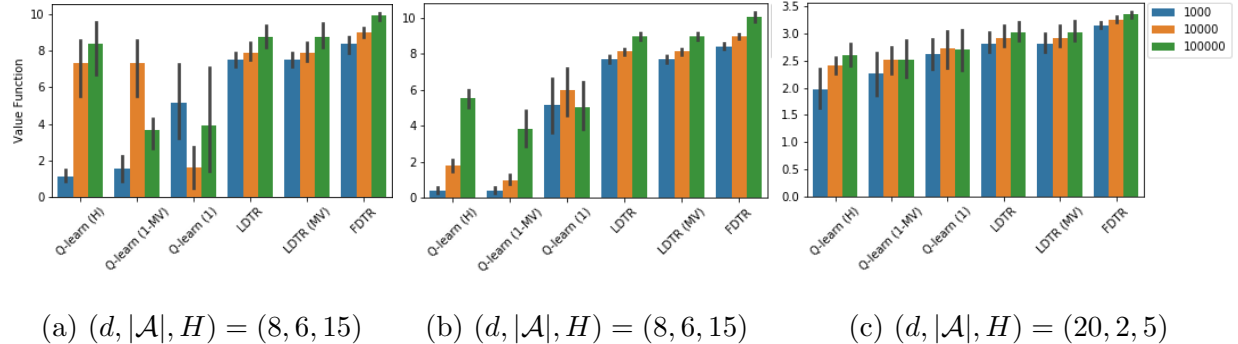


Figure 2: Mean value function for FDTR and benchmarks trained on $K = 5$ sites for plots 2a, 2c and $K = 10$ for plot 2b. We show value function estimates averaged over the K sites for increasing sample size. Error bars show 95% CI. Finally, $(d, |\mathcal{A}|, H)$ stands respectively for dimension of state space, cardinality of action space, and episode length.

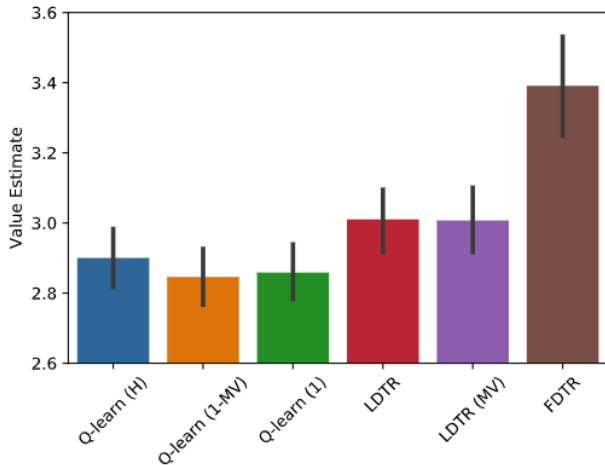


Figure 3: Value function estimates on the sepsis held out data across 10 ICUs.

Figure 2 shows empirical results for the performance of FDTR, the local and voting majority versions of our DTR approach, and their Q -learning counterparts for different setting configurations. It is clear that across settings, FDTR outperforms in terms of the mean value. These results are expected since FDTR is pulling data across sites to estimate the policy. As state dimension becomes large all methods decrease in performance for any given sample size, this is natural as estimated parameters have larger standard errors. In these cases such as Figure 2(c), FDTR is still performing best relative to local and majority voting methods. It is worth noting that the larger sample size benefits FDTR in terms of better policy estimation and also decreases uncertainty in terms of its performance, as illustrated by the narrower standard errors. Additionally, FDTR has the capacity to estimate coefficients at the hospital level, which other methods cannot do locally. Hospital-level covariate estimation allows FDTR to tailor the policy to local hospital characteristics, translating into a better policy function.

5.2 FDTR for Sepsis treatment Across Intensive Care Units

We further illustrate the performance of FDTR on a real data application. We focus on sepsis, a state of infection that overwhelms the body’s immune system. We use the MIMIC-IV (Johnson et al., 2020) sepsis data as it has become a common data set to evaluate RL algorithms relevant to healthcare (Raghu et al., 2017; Sonabend et al., 2020; Komorowski et al., 2018). The MIMIC-IV datamart is comprised of de-identified patient medical records treated in different intensive care units (ICU). We use patient trajectories corresponding to 9 different ICUs with 25,568 patient trajectories (episodes).

The ICU level covariates include an indicator for whether dialysis is ever used at the unit or oxygen saturation is ever measured for any patient in the unit. Patient-level covariates include measurements of weight, temperature, systolic blood pressure, and others. The state-space dimension is 14. Each time step consists of a four-hour interval, and trajectories consist of $H = 5$ time steps. The reward is proportionately inverse to the lactic acid level, and the action space corresponds to the dosage quartile for IV fluids yielding four different actions. We use a step-importance sampling estimator (Thomas and Brunskill, 2016; Gottesman et al., 2018) for the value function, which we use to compare methods. We use an 80%-20% split at each ICU for training and test data, respectively. We train all methods described in Section 5.1 and evaluate them at each data center. Figure 3 shows the value function estimate averaged over ICU test sets. Estimates are computed for all methods along with 95% CI. We can see a clear advantage of using a DTR-type approach. Not surprisingly, FDTR performs significantly better than the rest of the methods. The superior performance is because FDTR borrows information from across ICUs and can estimate ICU-specific covariates such as the use of dialysis, which yields a superior policy function.

6 Conclusion

Given the massive amount of healthcare data increasingly available across medical institutions, and the important privacy constraints these have, FDTR is an efficient way of collaboration that brings us closer to finding optimal treatment. The proposed FDTR algorithm effectively combine multi-site data to learn optimal policies for individual institutions while borrowing shared information across sites to improve efficiency. We prove the suboptimality of FDTR and demonstrate its effectiveness in simulations and comparing policies for sepsis treatment.

The currently implementation of FDTR allows users to specify features with common effects across sites and features with site-specific effects. It is also plausible to allow for more data-adaptive co-training by imposing shrinkage estimation on the learned site-specific parameters, following strategies similar to the heterogeneity-aware federated regression methods (Cai et al., 2021; Duan et al., 2022). We show the sample complexity of the FDTR will be comparable to the homogeneous case under our model and it is interesting to find if the sample complexity involving shrinkage estimation will have similar results.

A limitation of FDTR is that it assumes a linear MDP; this assumption can be strong when dealing with real-world applications. However, this limitation can be addressed using feature engineering designed with subject matter experts, i.e., ICU clinicians who treat sepsis. An interesting extension to our method would be to equip FDTR with doubly robust (DR) models. For example, if we additionally model the treatment propensity observed in the data, a DR version of FDTR could potentially achieve suboptimality even if the linear MDP assumption is incorrect. Another extension is to develop such communication-efficient and privacy-preserving FDTR algorithms for more general models, which warrants future exploration.

References

Agarwal, R., D. Schuurmans, and M. Norouzi (2020). An optimistic perspective on offline reinforcement learning. In *International Conference on Machine Learning*, pp. 104–114. PMLR.

Agu, E., P. Pedersen, D. Strong, B. Tulu, Q. He, L. Wang, and Y. Li (2013). The smartphone as a medical device: Assessing enablers, benefits and challenges. In *2013 IEEE International Workshop of Internet-of-Things Networking and Control (IoT-NC)*, pp. 48–52. IEEE.

Antos, A., C. Szepesvári, and R. Munos (2008). Fitted q-iteration in continuous action-space mdps. In J. Platt, D. Koller, Y. Singer, and S. Roweis (Eds.), *Advances in Neural Information Processing Systems*, Volume 20. Curran Associates, Inc.

Battey, H., J. Fan, H. Liu, J. Lu, and Z. Zhu (2018). Distributed testing and estimation under sparse high dimensional models. *Annals of statistics* 46(3), 1352.

Cai, T., M. Liu, and Y. Xia (2021). Individual data protected integrative regression analysis of high-dimensional heterogeneous data. *Journal of the American Statistical Association* 0(0), 1–15.

Cao, B., L. Zheng, C. Zhang, P. S. Yu, A. Piscitello, J. Zulueta, O. Ajilore, K. Ryan, and A. D. Leow (2017). Deepmood: modeling mobile phone typing dynamics for mood detection. In *Proceedings of the 23rd ACM SIGKDD International Conference on Knowledge Discovery and Data Mining*, pp. 747–755.

Chakraborty, B. (2013). *Statistical methods for dynamic treatment regimes*. Springer.

Chakraborty, B. and S. A. Murphy (2014). Dynamic treatment regimes. *Annual review of statistics and its application* 1, 447–464.

Chen, T., K. Zhang, G. B. Giannakis, and T. Basar (2018). Communication-efficient distributed reinforcement learning. *arXiv preprint arXiv:1812.03239*.

Duan, R., Y. Ning, and Y. Chen (2022). Heterogeneity-aware and communication-efficient distributed statistical inference. *Biometrika* 109(1), 67–83.

Duan, Y., Z. Jia, and M. Wang (2020). Minimax-optimal off-policy evaluation with linear function approximation. In *International Conference on Machine Learning*, pp. 2701–2709. PMLR.

Duchi, J. C., M. I. Jordan, and M. J. Wainwright (2014). Privacy aware learning. *Journal of the ACM (JACM)* 61(6), 1–57.

Elgabli, A., J. Park, A. S. Bedi, M. Bennis, and V. Aggarwal (2020). Gadmm: Fast and communication efficient framework for distributed machine learning. *Journal of Machine Learning Research* 21(76), 1–39.

Free, C., G. Phillips, L. Watson, L. Galli, L. Felix, P. Edwards, V. Patel, and A. Haines (2013). The effectiveness of mobile-health technologies to improve health care service delivery processes: a systematic review and meta-analysis. *PLoS Med* 10(1), e1001363.

Fujimoto, S., D. Meger, and D. Precup (2019). Off-policy deep reinforcement learning without exploration. In *International Conference on Machine Learning*, pp. 2052–2062. PMLR.

Gottesman, O., F. Johansson, M. Komorowski, A. Faisal, D. Sontag, F. Doshi-Velez,

and L. A. Celi (2019). Guidelines for reinforcement learning in healthcare. *Nature medicine* 25(1), 16–18.

Gottesman, O., F. Johansson, J. Meier, J. Dent, D. Lee, S. Srinivasan, L. Zhang, Y. Ding, D. Wihl, X. Peng, et al. (2018). Evaluating reinforcement learning algorithms in observational health settings. *arXiv preprint arXiv:1805.12298*.

Gulcehre, C., Z. Wang, A. Novikov, T. L. Paine, S. G. Colmenarejo, K. Zolna, R. Agarwal, J. Merel, D. Mankowitz, C. Paduraru, et al. (2020). RL unplugged: Benchmarks for offline reinforcement learning. *arXiv preprint arXiv:2006.13888*.

Hao, M., H. Li, X. Luo, G. Xu, H. Yang, and S. Liu (2019). Efficient and privacy-enhanced federated learning for industrial artificial intelligence. *IEEE Transactions on Industrial Informatics* 16(10), 6532–6542.

Hard, A., K. Rao, R. Mathews, S. Ramaswamy, F. Beaufays, S. Augenstein, H. Eichner, C. Kiddon, and D. Ramage (2018). Federated learning for mobile keyboard prediction. *arXiv preprint arXiv:1811.03604*.

Hong, C., E. Rush, M. Liu, D. Zhou, J. Sun, A. Sonabend, V. M. Castro, P. Schubert, V. A. Panickan, T. Cai, et al. (2021). Clinical knowledge extraction via sparse embedding regression (keser) with multi-center large scale electronic health record data. *NPJ digital medicine* 4(1), 1–11.

Jiang, N. and L. Li (2016). Doubly robust off-policy value evaluation for reinforcement learning. In *International Conference on Machine Learning*, pp. 652–661. PMLR.

Jin, Y., Z. Yang, and Z. Wang (2021). Is pessimism provably efficient for offline RL? In *International Conference on Machine Learning*, pp. 5084–5096. PMLR.

Johnson, A., L. Bulgarelli, T. Pollard, S. Horng, L. A. Celi, and R. Mark. (2020). MIMIC-IV (version 0.4). PhysioNet.

Johnson, A. E., T. J. Pollard, L. Shen, H. L. Li-Wei, M. Feng, M. Ghassemi, B. Moody, P. Szolovits, L. A. Celi, and R. G. Mark (2016). MIMIC-III, a freely accessible critical care database. *Scientific data* 3(1), 1–9.

Jordan, M. I., J. D. Lee, and Y. Yang (2019). Communication-efficient distributed statistical inference. *Journal of the American Statistical Association* 114(526), 668–681.

Kidambi, R., A. Rajeswaran, P. Netrapalli, and T. Joachims (2020). Morel: Model-based offline reinforcement learning. *Advances in Neural Information Processing Systems* 33, 21810–21823.

Komorowski, M., L. A. Celi, O. Badawi, A. C. Gordon, and A. A. Faisal (2018). The artificial intelligence clinician learns optimal treatment strategies for sepsis in intensive care. *Nature medicine* 24(11), 1716–1720.

Konečný, J., H. B. McMahan, F. X. Yu, P. Richtárik, A. T. Suresh, and D. Bacon (2016). Federated learning: Strategies for improving communication efficiency. *arXiv preprint arXiv:1610.05492*.

Lange, S., T. Gabel, and M. Riedmiller (2012). Batch reinforcement learning. In *Reinforcement learning*, pp. 45–73. Springer.

Lavori, P. W. and R. Dawson (2004). Dynamic treatment regimes: practical design considerations. *Clinical trials* 1(1), 9–20.

Levine, S., A. Kumar, G. Tucker, and J. Fu (2020). Offline reinforcement learning: Tutorial, review, and perspectives on open problems. *arXiv preprint arXiv:2005.01643*.

Li, W., F. Milletarì, D. Xu, N. Rieke, J. Hancox, W. Zhu, M. Baust, Y. Cheng, S. Ourselin, M. J. Cardoso, et al. (2019). Privacy-preserving federated brain tumour segmentation. In *International Workshop on Machine Learning in Medical Imaging*, pp. 133–141. Springer.

Lim, H.-K., J.-B. Kim, J.-S. Heo, and Y.-H. Han (2020). Federated reinforcement learning for training control policies on multiple iot devices. *Sensors* 20(5), 1359.

Liu, B., Q. Cai, Z. Yang, and Z. Wang (2019). Neural trust region/proximal policy optimization attains globally optimal policy. *Advances in Neural Information Processing Systems* 32, 10565–10576.

Luckett, D. J., E. B. Laber, A. R. Kahkoska, D. M. Maahs, E. Mayer-Davis, and M. R. Kosorok (2020). Estimating dynamic treatment regimes in mobile health using v-learning. *Journal of the American Statistical Association* 115(530), 692–706.

McMahan, B., E. Moore, D. Ramage, S. Hampson, and B. A. y Arcas (2017). Communication-efficient learning of deep networks from decentralized data. In *Artificial Intelligence and Statistics*, pp. 1273–1282. PMLR.

Min, X., B. Yu, and F. Wang (2019). Predictive modeling of the hospital readmission risk from patients' claims data using machine learning: a case study on copd. *Scientific reports* 9(1), 1–10.

Murphy, S. A. (2003). Optimal dynamic treatment regimes. *Journal of the Royal Statistical Society: Series B (Statistical Methodology)* 65(2), 331–355.

Murphy, S. A., M. J. van der Laan, J. M. Robins, and C. P. P. R. Group (2001). Marginal mean models for dynamic regimes. *Journal of the American Statistical Association* 96(456), 1410–1423.

Nadiger, C., A. Kumar, and S. Abdelhak (2019). Federated reinforcement learning for fast personalization. In *2019 IEEE Second International Conference on Artificial Intelligence and Knowledge Engineering (AIKE)*, pp. 123–127. IEEE.

Parbhoo, S., J. Bogojeska, M. Zazzi, V. Roth, and F. Doshi-Velez (2017). Combining kernel and model based learning for hiv therapy selection. *AMIA Summits on Translational Science Proceedings 2017*, 239.

Prasad, N., L.-F. Cheng, C. Chivers, M. Draugelis, and B. E. Engelhardt (2017). A reinforcement learning approach to weaning of mechanical ventilation in intensive care units. *arXiv preprint arXiv:1704.06300*.

Puterman, M. L. (2014). *Markov decision processes: discrete stochastic dynamic programming*. John Wiley & Sons.

Raghu, A., M. Komorowski, L. A. Celi, P. Szolovits, and M. Ghassemi (2017). Continuous state-space models for optimal sepsis treatment: a deep reinforcement learning approach. In *Machine Learning for Healthcare Conference*, pp. 147–163. PMLR.

Robins, J. M. (2004). Optimal structural nested models for optimal sequential decisions. In *Proceedings of the second seattle Symposium in Biostatistics*, pp. 189–326. Springer.

Roomi, S., S. O. Shah, W. Ullah, S. U. Abedin, K. Butler, K. Schiers, B. Kohl, E. Yoo, M. Vibbert, and J. Jallo (2021). Declining intensive care unit mortality of covid-19: a multi-center study. *Journal of clinical medicine research* 13(3), 184.

Scherrer, B., M. Ghavamzadeh, V. Gabillon, B. Lesner, and M. Geist (2015). Approximate modified policy iteration and its application to the game of tetris. *Journal of Machine Learning Research* 16, 1629–1676.

Sonabend, A., N. Laha, A. N. Ananthakrishnan, T. Cai, and R. Mukherjee (2020). Semi-

supervised off policy reinforcement learning. *arXiv preprint arXiv:2012.04809*.

Sonabend, A., J. Lu, L. A. Celi, T. Cai, and P. Szolovits (2020). Expert-supervised reinforcement learning for offline policy learning and evaluation. In *Advances in Neural Information Processing Systems*, Volume 33, pp. 18967–18977.

Steinhubl, S. R., E. D. Muse, and E. J. Topol (2013). Can mobile health technologies transform health care? *Jama* 310(22), 2395–2396.

Sutton, R. S. and A. G. Barto (2018). *Reinforcement learning: An introduction*. MIT press.

Thomas, P. and E. Brunskill (2016). Data-efficient off-policy policy evaluation for reinforcement learning. In *International Conference on Machine Learning*, pp. 2139–2148. PMLR.

Wang, X., Z. Yang, X. Chen, and W. Liu (2019). Distributed inference for linear support vector machine. *Journal of Machine Learning Research* 20.

Xu, X., H. Peng, L. Sun, M. Z. A. Bhuiyan, L. Liu, and L. He (2021). Fedmood: Federated learning on mobile health data for mood detection. *arXiv preprint arXiv:2102.09342*.

Yang, Q., Y. Liu, T. Chen, and Y. Tong (2019). Federated machine learning: Concept and applications. *ACM Transactions on Intelligent Systems and Technology (TIST)* 10(2), 1–19.

Zhang, K., Z. Yang, and T. Başar (2019). Multi-agent reinforcement learning: A selective overview of theories and algorithms. *arXiv preprint arXiv:1911.10635*.

Zhang, R., B. Dai, L. Li, and D. Schuurmans (2020). Gendice: Generalized offline estimation of stationary values. *arXiv preprint arXiv:2002.09072*.

Zhang, Z., B. Zheng, and N. Liu (2020). Individualized fluid administration for critically ill patients with sepsis with an interpretable dynamic treatment regimen model. *Scientific Reports* 10(1), 1–9.

Zhuo, H. H., W. Feng, Q. Xu, Q. Yang, and Y. Lin (2019). Federated reinforcement learning. *arXiv preprint arXiv:1901.08277*.